Have mailed other copies to R.C. B. This is corrected copy. Thor

EXPERIMENTAL INVESTIGATION OF RESONANCE SELF-SHIELDING AND THE DOPPLER EFFECT IN URANIUM AND TANTALUM*

Tae Y. Byoun+ and R. C. Block
Rensselaer Polytechnic Institute

and

++ T. T. Semler
NASA Lewis Research Center.

Submitted for outside publication in a Journal

*Work Supported by NASA Grant NGR 33-018-134

+In partial fulfillment for the degree of Doctor of Philosophy

++ Presently employed by Aerospace Research Applications Center, Indiana University, Bloomington, Indiana 47401

96

ABSTRACT

A series of average transmission and average self-indication ratio measurements have been performed in order to investigate the temperature dependence of the resonance self-shielding effect in the unresolved resonance region of depleted uranium and tantalum. The measurements were carried out at $77^{o}K$, $295^{o}K$ and $\approx 1000^{o}K$ with sample thicknesses varying from ~0.1 to ~1.0 mean free path. The average resonance parameters as well as the temperature dependence have been determined by using an analytical model which directly integrates over the resonance parameter distribution functions.

INTRODUCTION

The main contribution of the Doppler effect in a fast breeder reactor comes from "the unresolved resonance region"[1] where the detailed resonance structure has not been, and possibly cannot be, experimentally determined. The temperature variation of the neutron flux inside the reactor must be predicted for safe reactor ~~operation.~~ design The prediction of this temperature-dependent variation of neutron flux follows from:

1) the determination of the average resonance parameters with which the cross section and resonance structure can be reproduced (or at least simulated),

2) sufficient knowledge about the temperature dependence of the resonance self-shielding effect based on the above average parameters.

In order to predict the cross section in the unresolved region it is necessary to assume that the resonance parameters are governed by some specified statistical distribution functions (such as the Wigner level spacing distribution[2] and the Porter-Thomas neutron width distribution[3]). Furthermore it is necessary to assume that the average resonance parameters determined in the resolved region can be extrapolated into the unresolved region. One of the main purposes of this investigation is the establishment of the validity in extrapolating the low energy parameters of Ta and depleted U into the unresolved region, using only a single level formalism.

One of the best ways to achieve the above goal is to perform

a series of direct measurements on a system with good geometry and to obtain as many sets of data as possible by varying sample temperature and thickness. The average self-indication ratio, <SIR>, and the average transmission, <TR>, measurements were selected for the experimental investigation of the Doppler effect in the unresolved region. Reviewing previous temperature-dependent measurements, no <SIR> measurements have been reported although the data from <TR> measurements[4,5] are presently available. This is due to the difficulty arising from the unusually large background-to-signal ratio in the <SIR> measurements. The experiments undertaken here are the first to attempt direct measurements by combining both <TR> and <SIR> methods.

These data were analyzed by using both a statistical sampling method[6,7] and an analytical method.[8,9] The results obtained by using the statistical method (computer code DAISY[6]) have been presented in previous publications[8,10,10a] with somewhat different conclusions, and will not be presented here. Both the ideal gas model and the Lamb effective temperature model[11] were applied and compared.

EXPERIMENTAL TECHNIQUE

Most of the aspects of the experimental technique have been described in previous reports[8,10] and are briefly summarized here. The RPI linear accelerator was used to produce neutrons for the time-of-flight experiment. The accelerator was operated at an electron energy 70 MeV, a repetition rate 480 pps and with an electron pulse width of 20 to 250 nanoseconds.

A ^{10}B-NaI detector at a 28 meter flight path and a large scintillator detector at 25.69 meters were used along with a PDP-7 on-line computer for data acquisition.

The self-indication experiment along with a typical self-indication spectra (for the 66.1 eV resonance) are illustrated in Figure 1a and 1b. These measurements were performed at 77^{+5o}_{-1}K and 295 ± 2^{o}K for both tantalum and depleted uranium (99.8% ^{238}U and 0.2% ^{235}U) and 973 ± 5^{o}K for depleted uranium (1073 ± 5^{o}K for tantalum) varying the sample thickness from ~0.1 to ~1.0 mean free path. The overall view of the electronics and the data acquisition system are shown in Figure 1c. An evacuated furnace and a liquid-nitrogen cryostat were used to obtain high temperature samples and for low temperature samples, respectively. An automatic sample cycling system was utilized to alternate sample "into" and "out of" the neutron beam. The capture sample inside the self-indication detector was kept at room temperature throughout the self-indication experiments.

The average self-indication ratio, <SIR>, and the average transmission, <TR>, are defined as:

$$\langle SIR \rangle = \frac{\int_{\Delta E} Y_\gamma(E,T_2 n_2)\exp[-n_1\sigma_t(E,T_1)]dE}{\int_{\Delta E} Y_\gamma(E,T_2,n_2)dE} \qquad (1)$$

$$\langle TR \rangle = \frac{1}{\Delta E}\int_{\Delta E}\exp[-n_1\sigma_t(E,T_1)]dE \qquad (2)$$

where the subscripts 1 and 2 indicate the shielding and self-

indication samples, respectively. The sample temperature, and sample thickness are denoted by T and n. The capture yield,[12] Y_γ, can be approximated by $Y_\gamma \approx n_2 \sigma_\gamma$ for $n_2 \ll 1$.

ANALYSIS

The data were averaged over 10%-wide energy bins after dead-time and background corrections were made. The counting statistics (in standard deviations) of the experimental results are typically $\pm$ 1% in <TR> and $\pm$ 2% in <SIR>. Since very thin self-indication samples (0.00147 atom/barn for Ta and 0.00379 atom/barn for depleted uranium) were used, the multiple scattering effects in calculating <SIR> can be neglected in the unresolved resonance region.[10]

The analytical method has been developed and applied to interpret the data. In this method, the expressions for <TR> and <SIR> in Eqs. (1) and (2) are separated into two parts: the unshielded term and the shielded term. Assuming that $|\sigma_t - \langle\sigma_t\rangle| < 1/n_1$ and $n_2 \ll 1$, the definitions of <TR> and <SIR> in eqs. (1) and (2) become

$$\langle SIR \rangle = \frac{e^{-n_1\langle\sigma_t\rangle}}{\langle\sigma_\gamma\rangle} \langle \sigma_\gamma e^{-n_1(\sigma_t - \langle\sigma_t\rangle)} \rangle \qquad (3)$$

$$\langle TR \rangle = e^{-n_1\langle\sigma_t\rangle} \langle e^{-n_1(\sigma_t - \langle\sigma_t\rangle)} \rangle \quad , \qquad (4)$$

where <...> stands for the average over the energy interval, ΔE. Doppler broadened total and radiative capture cross sections are

denoted by σ_t and σ_γ, respectively.

The second terms in eqs. (3) and (4) are defined as the self-shielding factors η_{SIR} and η_{TR}, and the exponential expressions appearing in η_{SIR} and η_{TR} are expanded into four terms:[8,9]

$$\eta_{TR} \equiv \langle e^{-n_1(\sigma_t - \langle\sigma_t\rangle)} \rangle \tag{5}$$

$$\approx 1 + \frac{1}{2} n_1^2 \langle(\sigma_t - \langle\sigma_t\rangle)^2 - \frac{1}{6} n_1^3 \langle(\sigma_t - \langle\sigma_t\rangle)^3\rangle \tag{5}'$$

$$\eta_{SIR} \equiv \langle\sigma_\gamma e^{n_1(\sigma_t - \langle\sigma_t\rangle)} \rangle \tag{6}$$

$$\approx \langle\sigma_\gamma\rangle - n_1\langle\sigma_\gamma(\sigma_t - \langle\sigma_t\rangle)\rangle + \frac{1}{2} n_1^2 \langle\sigma_\gamma(\sigma_t - \langle\sigma_t\rangle)^2\rangle - \frac{1}{6} n_1^3 \langle\sigma_\gamma(\sigma_t - \langle\sigma_t\rangle)^3\rangle \tag{6}'$$

where the linear term in eq. (5)' vanishes since $\langle(\sigma_t - \langle\sigma_t\rangle)\rangle = 0$.

The self-shielding factors are functions of the average cross sections $\langle\sigma_\gamma\rangle$ and $\langle\sigma_t\rangle$, the variance term $\langle(\sigma_t - \langle\sigma_t\rangle)^2\rangle$, the triance term $\langle(\sigma_t - \langle\sigma_t\rangle)^3\rangle$, and the values of these respective terms weighted by the capture cross section. Since the evaluation of these terms by energy integration is impossible without the detailed information about point-wise cross sections in the unresolved region, the energy integrations were replaced by the integrations over the corresponding statistical distribution functions: viz. the Wigner level

spacing distribution[2] and the Porter-Thomas neutron width distribution functions.[3] This analytical model which directly integrates over the statistical distribution functions is 10^2 to 10^3 faster in computation time than the statistical sampling method.[6] The Breit-Wigner single level formula was used for s- and p-wave cross sections. The cross section overlapping effects of the same resonance sequences as well as the different resonance sequences were considered. The details of the analytical method have been presented elsewhere.[8,9] For given sets of average resonance parameters, <TR> and <SIR> were calculated and compared with experimental values for different sample thicknesses, energy intervals, and sample temperatures.

The multi-level effects which can be significant in the fissile nuclides and medium-weight nuclei were not considered. However, the experimental evidence shows that the influence of multi-level effects on the temperature dependence is almost negligible.[13]

DEPLETED URANIUM RESULTS

A) Average Resonance Parameters

The average resonance parameters which best fit the experimental results (<TR> and <SIR>) in the energy range of 10 to 100 keV are tabulated in Table I. In Figures 2a and 2b the results are plotted in terms of <SIR> and <TR>, and the comparison of these results with the ENDF/B-III evaluated parameters is given. In Figures 3a and 3b the average total and capture cross sections calculated using the above parameters (denoted by grand average parameters in the figures) are compared with those cal-

culated using the local average parameters which best fit the <TR> and <SIR> of each 10%-wide energy bin for five different sample thicknesses.

The p-wave strength function, S_1, which best fits the experimental results ranges from 1.27×10^{-4} to 2.4×10^{-4} for corresponding variations of the scattering length, R', ranging from 9.0 to 9.6 fermis. Since the potential cross section, σ_p, calculated from these values of R' (σ_p = 10.0 barns for R' = 9.0 fm and σ_p = 11.4 barns for 9.6 fm at 10 keV), are within the error limitations of measured values,[14,15] the choice of any set of parameters (labeled A,B, or C in Table I) can be made only if the potential cross section data are improved further. The sensitivity of <TR> and <SIR> to the changes in R', strength functions, and level spacings are shown in Figures 4a, 4b and 4c. According to Figure 4b, the <SIR> is more sensitive to the change in p-wave strength function, S_1, while the <TR> is more sensitive to the change in s-wave strength function, S_o. This makes the <SIR> experiment a powerful method for a determination of both s- and p-wave resonance parameters when combined with the <TR> experiment.

It should be noticed that the <SIR> of the depleted uranium could not have been fit well by using the conventional $(2J+1)^{-1}$-dependence formula for the level spacing which assumes parity independence.[16] The best-fit p-wave level spacing, $\langle D_1 \rangle$ is 11.3 ± 3.0 eV, which is approximately 60% larger than $\langle D_1 \rangle$ calculated from $\langle D_o \rangle$ according to $(2J+1)^{-1}$-dependence formula for $\langle D_{\ell J} \rangle$. This could indicate that there is parity dependence of

level spacing. The fit obtained using the ENDF/B-III parameters ($\langle D_1 \rangle$ = 6.67 eV and labeled (D) in Figure 2a) predicts consistently higher (2 to 7%) values of <SIR> than the experimental results. Yet the prediction of <TR> by the ENDF/B-III parameters is in excellent agreement with experimental <TR> as shown in Figure 2b. However, it is difficult to conclude that there is a definite parity dependence because of the possible uncertainties involved in the calculations (the neglect of the d-wave contribution, the theoretical ambiguity about J-dependence of strength functions and the experimental errors). The experimental errors in <SIR> are typically $\pm$ 2.0% due to counting statistics and $\pm$ 2.0% due to estimated systematic components.

B) Temperature Dependence of <TR> and <SIR>

Both the ideal gas model and the Lamb effective temperature model[11] have been applied to calculate <TR> and <SIR>, and the comparison is shown in Table II. For a sample temperature of 77°K, the ideal gas model predicts a slightly larger <TR> and a lower <SIR> because of the larger cross-section fluctuation predicted by this model. However, the difference between the predictions of two models is negligible above room temperature.

The self-shielding effect in <TR> and <SIR>, as can be seen in Eqs. 3 and 4, depends on:

1) cross-section fluctuations,

2) sample temperature,

3) sample thickness.

In general, the cross-section fluctuations decrease as the

neutron energy increases because of the decrease in peak cross sections, the increase in neutron width and the decrease in level spacing. The cross-section fluctuations also decrease as temperature increases due to the Doppler effect. Therefore, the <TR> and <SIR> both become smaller for lower neutron energies and for higher sample temperatures. These effects are also correlated with the thicknesses of the shielding samples. At the peak of a resonance, both <TR> and <SIR> increase with temperature because of the decrease in peak cross section at higher temperature. This effect is reversed at the wings of a resonance. If a shielding sample is thick enough to 'saturate' the transmission in the vicinity of a resonance peak, then <TR> and <SIR> decrease with temperature; this is especially noticeable at low energies below 2 keV. As the sample becomes thicker, the 'transmission saturation' effect in the vicinity of a resonance peak becomes severe, causing a smaller temperature effect for thicker samples than expected. This is shown in Table III in the energy range of 200 eV to 300 eV for both <TR> and <SIR> of depleted uranium. As the neutron energy increases the 'transmission saturation' effect decreases so that the contribution from the resonance peak to <TR> and <SIR> becomes larger. This effect can be seen in Figure 5a where the cold-to-room <SIR> ratio decreases as neutron energy increases due to an increasing resonance-peak contribution at higher energies.

The thermal expansion of the sample thickness also plays an important role in the temperature-dependence of <TR> and <SIR>.

Since the sample becomes effectively thinner at higher temperature, the <TR> and <SIR> increase with temperature as can be seen in Table III. Here, in the energy range of 20 to 30 keV, the observed cold-to-room and room-to-hot ratios (shown in parentheses) are less than unity because of thermal expansion of the samples.

TANTALUM RESULTS

The average resonance parameters from the analytical method which best fit the <TR> and <SIR> of tantalum in the energy range of 10 to 100 keV are listed in Table IV. In Figures 6a and 6b the <SIR> and <TR> based on these parameters are shown and compared with the experimental values for different sample thicknesses. The temperature dependences of <TR> and <SIR> of tantalum are essentially analogous to those of depleted uranium and the details of results have been reported elsewhere.[10] However the analytic technique used herein is performed neglecting the effect of the different spin states of tantalum.

The best-fit s-wave level spacing, $\langle D_o \rangle$, was $4.3^{-0.5}_{+1.5}$ eV, and corresponding p-wave level spacing, $\langle D_1 \rangle$, was $2.15^{-0.25}_{+0.35}$ eV. The potential cross section obtained using the scattering length, R' = 8.19 fermis, ranges from 8.42 barns at 1.0 keV to 7.8 barns at 100 keV, both of which are slightly higher than the measured low energy value of 7.0 + 1.0 barns.[17] The best-fit s-wave strength function (in the energy range of 10 to 100 keV), $S_o = 1.6^{+3.0}_{-0.2}$ (10^{-4}), is slightly lower than the previously measured values, which range from 1.8×10^{-4} (with Γ_γ = 0.055 eV and $\langle D_o \rangle$ = 4.3 eV)[18] to 2.0×10^{-4} (with Γ_γ = 0.065 eV, $\langle D_o \rangle$ = 4.3 eV and $S_1 = 0.2 \times 10^{-4}$)[19]. However, it appears that in the energy range

from 1 keV to 10 keV, a slightly higher s-wave strength function ($S_o = 2.0 \times 10^{-4}$) fits both <TR> and <SIR> better for the thinnest sample (Figures 6a and 6b).

The applicability of the analytical model depends on the sample thickness, the cross section fluctuations and the sample temperature. As can be seen in Figures 6a and 6b (and also in Figure 2), for the thickest sample (0.0802 atom/barn) the analytical model fails to predict <TR> and <SIR> at the energies below ~13 keV, while the analytical model continues to work at the energies down to ~1 keV for the thinnest sample (0.00563 atom/barn). This is expected since the exponent, $n_1\sigma_t$, appearing in the expressions of <TR> and <SIR> in Eqs. (3) and (4) becomes larger at lower energies and for thicker samples, and the four-term approximation begins to break down.

In Figure 7, the self-shielding factors calculated from <TR> and <SIR>, η_{TR} and η_{SIR}, are compared in terms of the average effective (shielded) cross sections,[20] $\langle\sigma\rangle_{TR}^{eff}$ and $\langle\sigma\rangle_{SIR}^{eff}$. In general, η_{TR} is greater than or equal to unity, and as long as the potential-to-resonance interference effects of the elastic scattering cross section do not dominate, η_{SIR} is less than or equal to unity;[20] that is,

$$\eta_{SIR} \leq 1 \leq \eta_{TR}$$

Therefore, $\langle\sigma\rangle_{SIR}^{eff}$ is greater than or equal to the true average total cross section while this effect is reversed for $\langle\sigma\rangle_{TR}^{eff}$, i.e.,

$$\langle\sigma\rangle_{TR}^{eff} \leq \langle\sigma_t\rangle \leq \langle\sigma\rangle_{SIR}^{eff}$$

Figure 7 also shows that the self-shielding effect becomes smaller (the value, $|1-\eta|$, becomes smaller) as the neutron energy increases and the difference between $\langle\sigma\rangle_{TR}^{eff}$ and $\langle\sigma\rangle_{SIR}^{eff}$ decreases.

CONCLUSIONS

This work represents an extensive investigation of the energy and temperature dependence of depleted uranium and tantalum in the unresolved resonance region. The analytical model has been developed for the interpretation of the data in the unresolved region. The results of this investigation are graphically summarized in Figures 2 to 7 and are listed in Tables I and IV. The general concluding remarks which follow from these are:

1) The average resonance single level parameters of both depleted uranium and tantalum in the energy range 10 keV to 100 keV have been determined and compared with other measurements (Tables I and IV). These parameters which best fit <TR> and <SIR> agree with low energy parameters within the statistical counting error limitations for both samples, establishing the validity of the single level extrapolation of the resolved region parameters into the unresolved resonance region.

2) The <SIR> is more sensitive to σ_γ and to p-wave resonance parameters, while the <TR> is more sensitive to σ_t and s-wave resonance parameters. The combination of <SIR> and <TR> experiments provides a comprehensive determination of the key parameters necessary to carry out reactor calculations in the unresolved region.

3) The applicability of the analytical model can be extended to lower energies if the sample thickness is optimized in the measurements. Since the average quantities appearing in the <TR> and <SIR> are calculated by direct integration over the known statistical distribution functions, the analytical model has a great advantage over the statistical sampling method in calculation time. The analytical method is 10^2 to 10^3 faster than the statistical sampling method. ~~This method extracts the average resonance parameters for single-level Breit-Wigner formalisms so that the results can be directly used in reactor calculations~~.

4) The <TR> and <SIR> decrease as temperature increases in the energy region below ~5 keV for both the uranium and tantalum. However, at higher energies the <SIR> increases with temperature and energy, while the <TR> continues to decrease as temperature increases. The 'transmission saturation' effect at the resonance peak as a function of the sample thickness plays an important role for the temperature dependence of the <TR> and <SIR> .

5) The ideal gas model predicts a slightly larger <TR> and a lower <SIR> than the predictions by the Lamb effective model. However, the difference in predictions between two models is negligible above room temperature.

REFERENCES

1. R. C. Block, "Neutron Cross Section Measurements Spanning the Resolved-to-the-Unresolved Resonance Region," Invited Paper, ANS Meeting, Toronto, June 1968.
2. E. P. Wigner, ORNL Report No. 2309 (1956), unpublished.
3. C. E. Porter and R. G. Thomas, Phys. Rev., 104, 483 (1956).
4. O. D. Simpson and L. G. Miller, Nucl. Instr. and Meth., 61, 245 (1968), and "Studies of Unresolved Resonances with a 2 keV Beam," CNA Meeting, Toronto, Canada, June 1968.
5. A. A. Van'kov, Yu. V. Grigor'yev, M. N. Nikolayev, V. V. Filippov, B. Bemer, S. Collatz and L. B. Pikel'ner, NASA TT F-13,693 (1971).
6. T. Semler, NASA TN D-5837 (1970).
7. M. W. Dyos, Nucl. Sci. Eng., 34, 181 (1969).
8. T. Y. Byoun, R. C. Block and T. Semler, CONF-720901 (Book 2), ANS Topical Meeting on New Development in Reactor Physics and Shielding, p. 1115, September 1972.
9. T. Y. Byoun, "Experimental Investigation of Resonance Self-Shielding and Doppler Effect in Uranium and Tantalum," Ph.D. Thesis, RPI, 1973.
10. T. Y. Byoun, R. C. Block and T. Semler, CONF-710301 (Vol. 2) 3rd Conf. Neutron Cross Section and Technology, 895 (1971).
11. W. E. Lamb, Phys. Rev., 55, 190 (1939).
12. J. A. Harvey, Ed., Experimental Neutron Resonance Spectroscopy, Chapter III (by E. R. Rae and R. C. Block), p. 155, Academic Press, New York (1970).

REFERENCES (Continued)

13. E. Schneider and F. H. Fröhner, IAEA-CN-26/10, 201 (1972).

14. J. E. Lynn, Proc. Phys. Soc., 82, 903 (1963).

15. F. Rahn, H. S. Camarda, G. Hacken, W. W. Havens, Jr., M. I. Liou, J. Rainwater, M. Slagowitz and S. Wynchank, Phys. Rev., C6, 1854 (1972).

16. A. Gilbert and A. G. W. Cameron, Can. J. Phys., 43, 1446 (1965).

17. R. E. Wood, Phys. Rev., 104, No. 5 (1956).

18. J. C. Desjardins, J. L. Rosen, W. W. Havens and J. Rainwater, Phys. Rev., 120, 2214 (1960).

19. J. H. Gibbons, EANDC 1961 (Neut. TOF Method), p. 151.

20. T. Y. Byoun and R. C. Block, RPI-328-187, 32 (1970).

FIGURE CAPTIONS

Figure 1a The Self-Indication Experiment Illustrated.

1b A Typical Self-Indication Spectrum of Depleted Uranium for Different Sample Thicknesses near the 66.1 eV Resonance.

1c The Overall View of Data Acquisition System.

Figure 2a, 2b Depleted Uranium <SIR> and <TR> Compared with the Analytical Calculations (See Table I for the average resonance parameter sets labeled A, B. C and D).

Figure 3a, 3b Average Total and Capture Cross Sections of Depleted Uranium.

Figure 4a The Sensitivity of <TR> and <SIR> to the Change of the Scattering Length, R'.

4b The Sensitivity of <SIR> and <TR> to the Change of the Strength Functions.

4c The Sensitivity of <SIR> and <TR> to the Change of the Level Spacings.

Figure 5a, 5b The Cold-to-Room Ratio of <TR> and <SIR> for Depleted Uranium of 0.03155 and 0.06206 atom/barn.

Figure 6a, 6b Tantalum <SIR> and <TR> Compared with the Analytical Calculations.

Figure 7 Effective Average Cross Sections of Tantalum Calculated from <SIR> and <TR>.

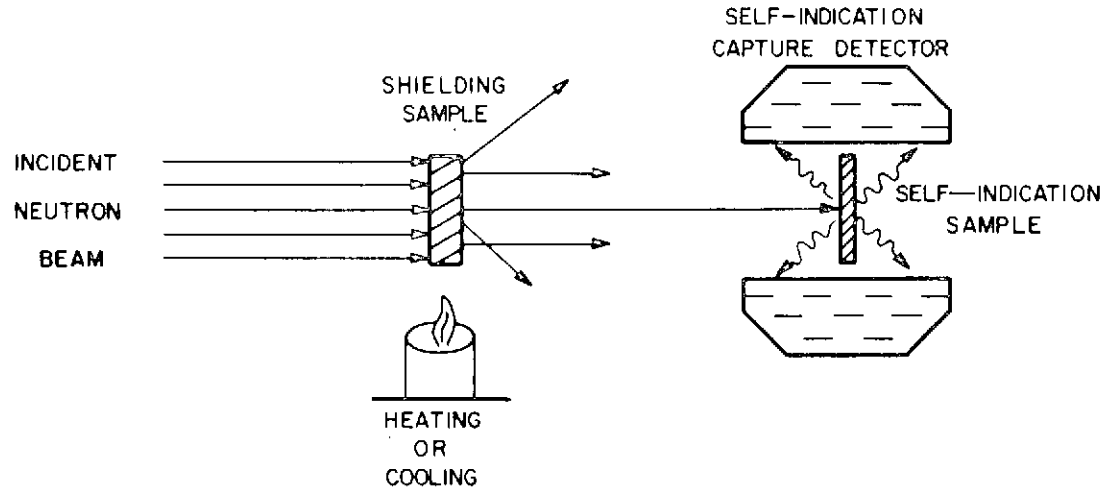

Figure 1a

SELF—INDICATION EXPERIMENT

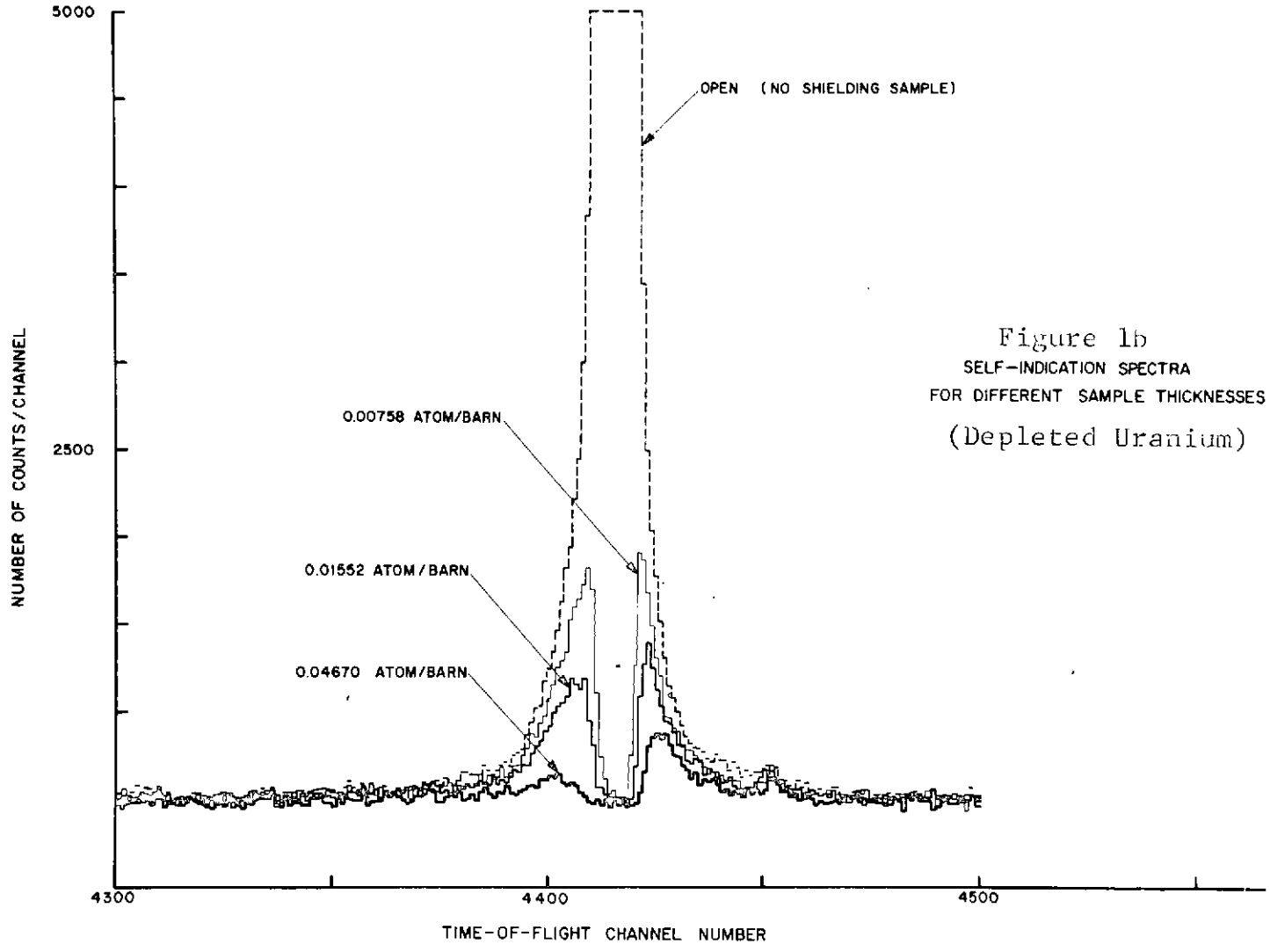

Figure 1b
SELF-INDICATION SPECTRA
FOR DIFFERENT SAMPLE THICKNESSES
(Depleted Uranium)

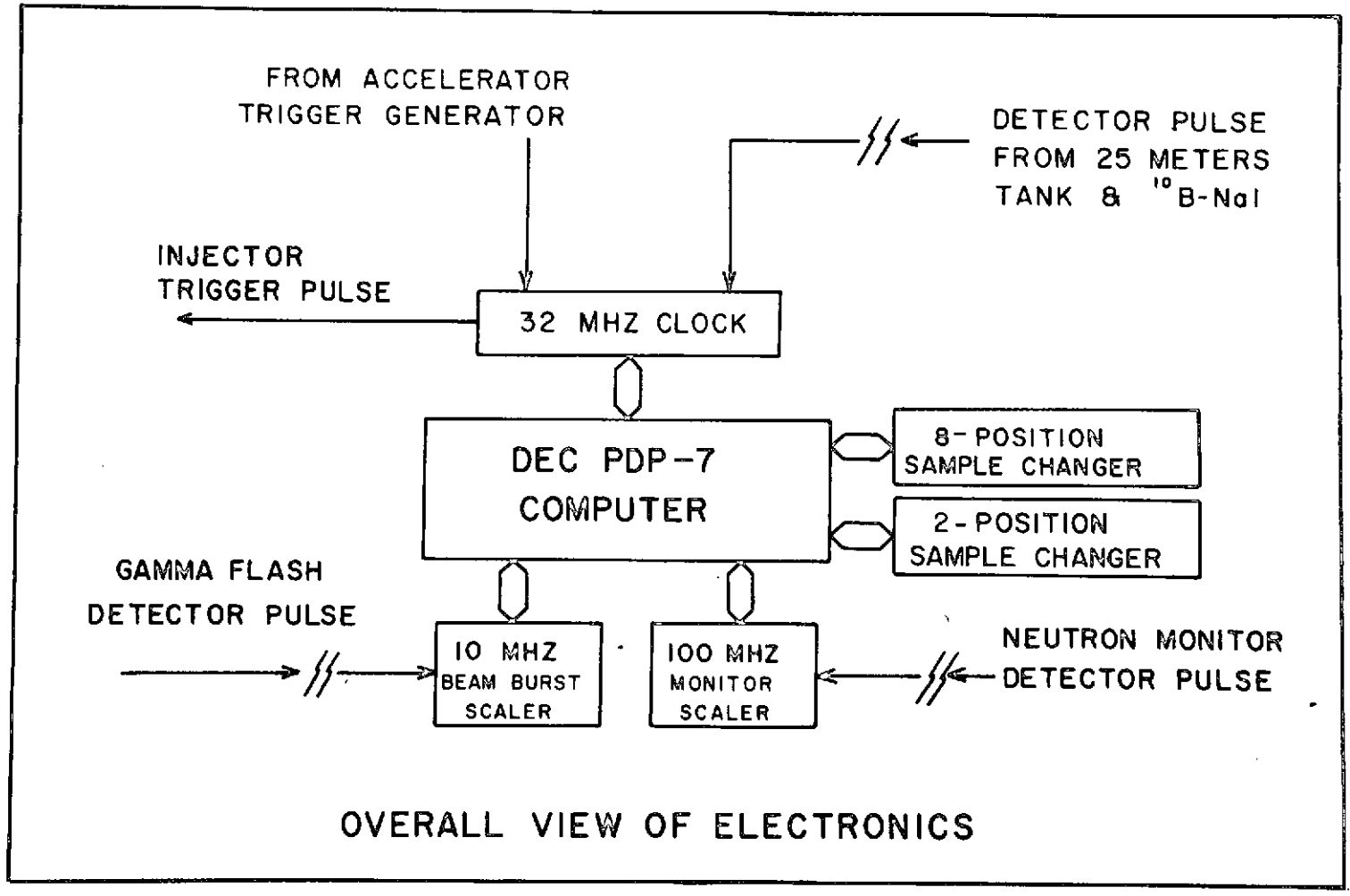
FROM ACCELERATOR
TRIGGER GENERATOR
DETECTOR PULSE
FROM 25 METERS
TANK & ^{10}B-NaI
INJECTOR
TRIGGER PULSE
32 MHZ CLOCK
DEC PDP-7
COMPUTER
8-POSITION
SAMPLE CHANGER
2-POSITION
SAMPLE CHANGER
GAMMA FLASH
DETECTOR PULSE
10 MHZ
BEAM BURST
SCALER
100 MHZ
MONITOR
SCALER
NEUTRON MONITOR
DETECTOR PULSE
OVERALL VIEW OF ELECTRONICS

Figure 1c

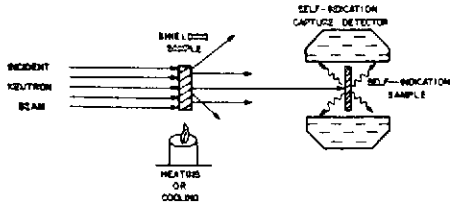

SELF-INDICATION EXPERIMENT

Figure Ia

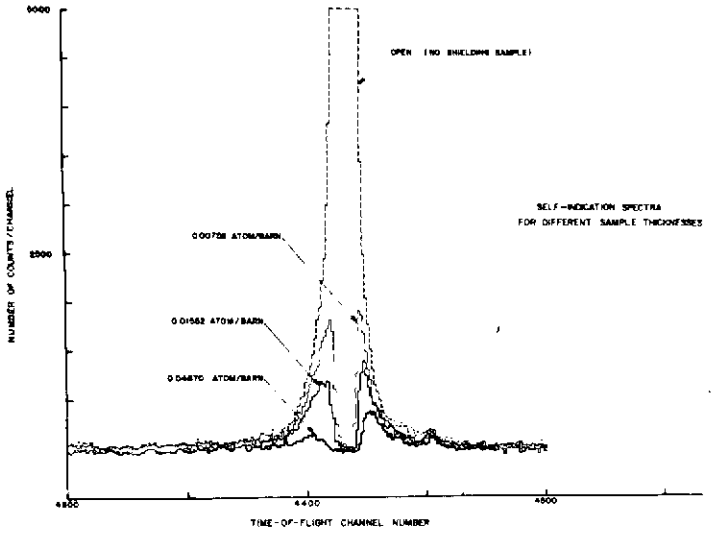

Figure Ib

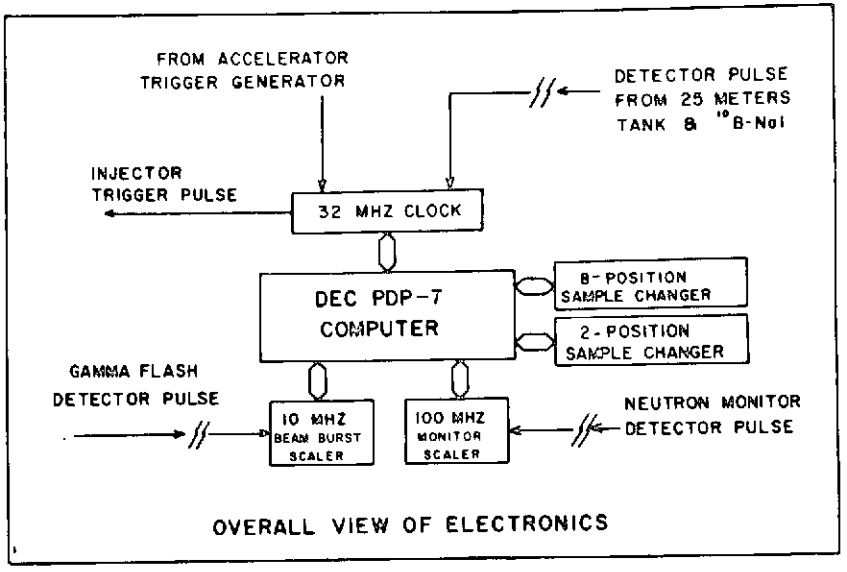

Figure Ic

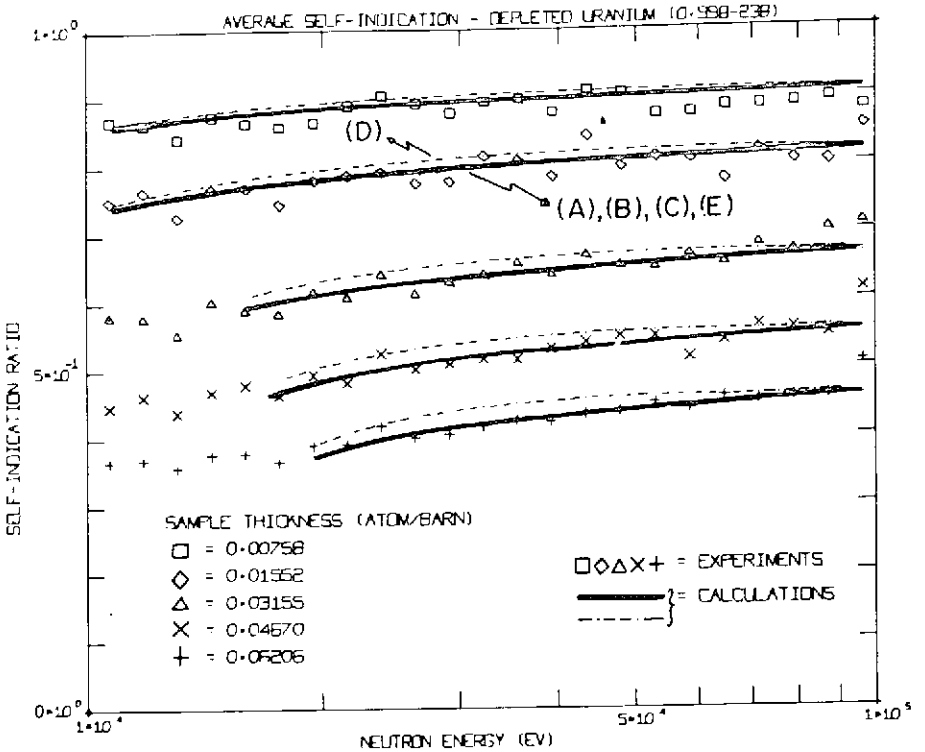

Figure 2a

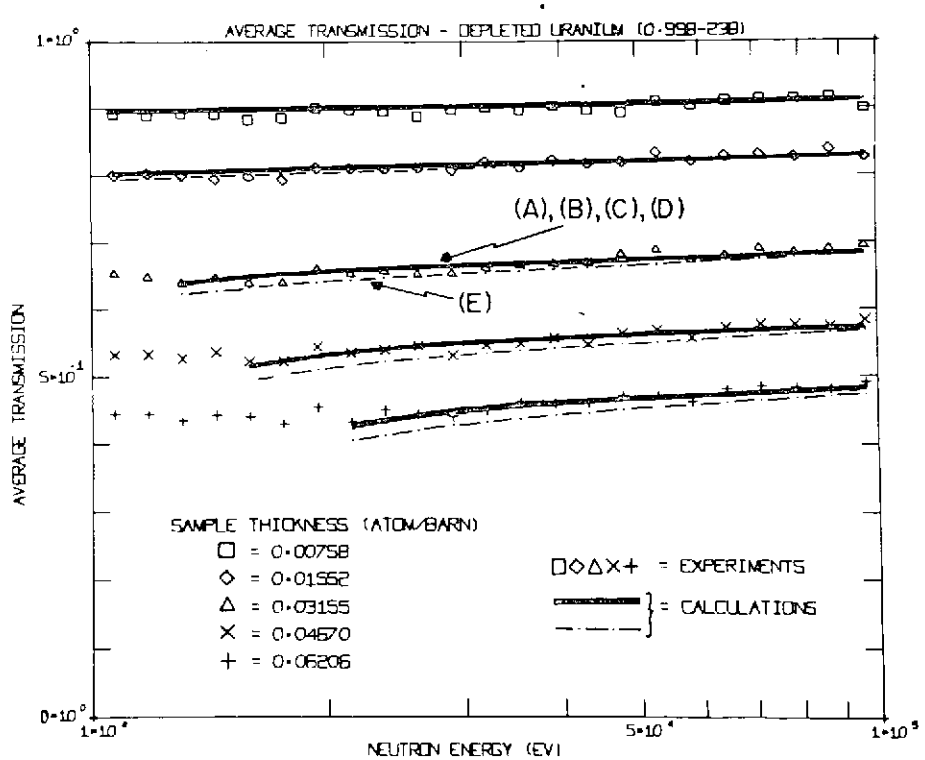

Figure 2b

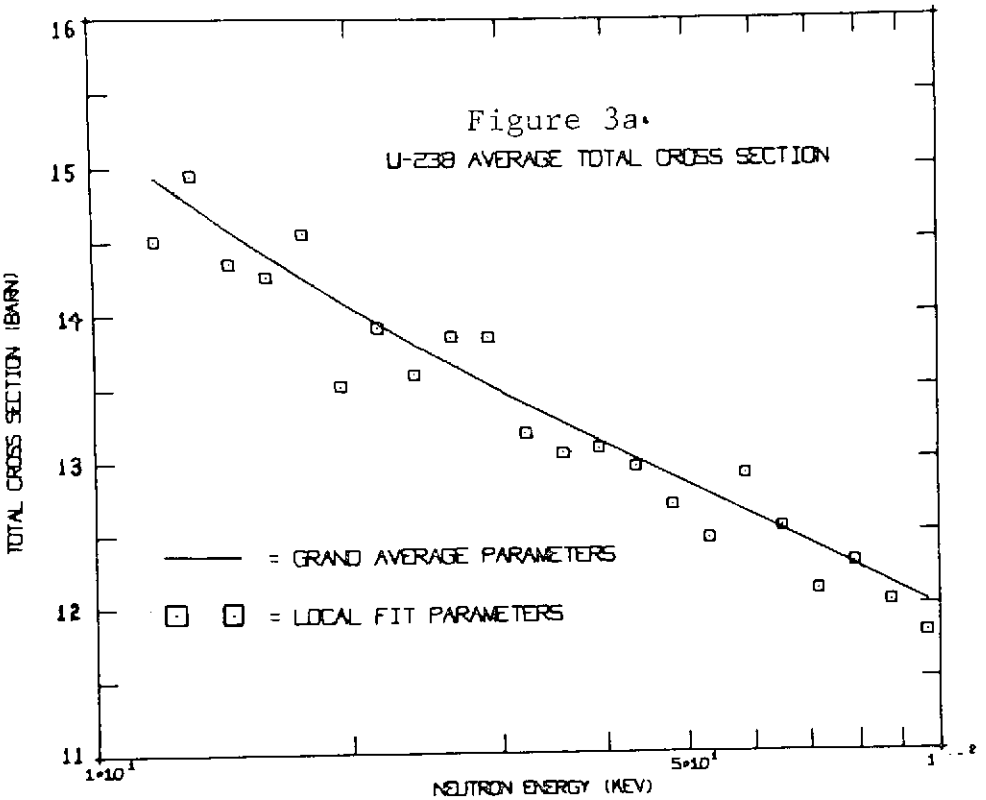
Figure 3a.
U-238 AVERAGE TOTAL CROSS SECTION
TOTAL CROSS SECTION (BARN)
16
15
14
13
12
11
= GRAND AVERAGE PARAMETERS
= LOCAL FIT PARAMETERS
1·10⁴
5·10⁴
1
NEUTRON ENERGY (KEV)

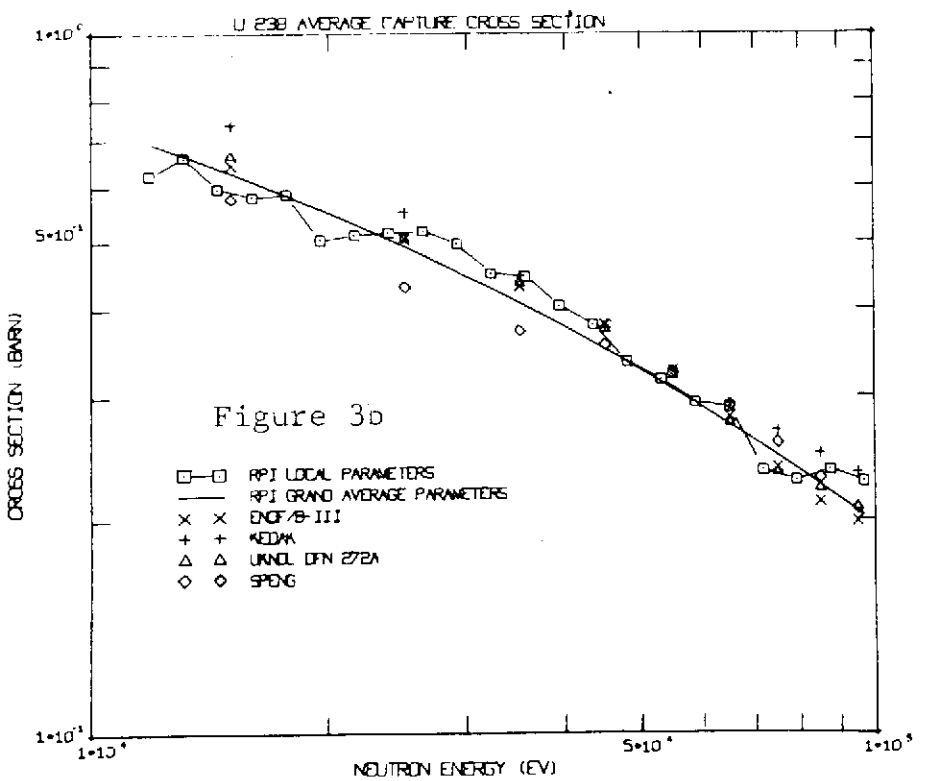
U 238 AVERAGE CAPTURE CROSS SECTION
CROSS SECTION (BARN)
1·10⁰
5·10⁻¹
1·10⁻¹
1·10⁴
5·10⁴
1·10⁵
NEUTRON ENERGY (EV)
Figure 3b
RPI LOCAL PARAMETERS
RPI GRAND AVERAGE PARAMETERS
ENDF/B-III
KEDAK
UKNDL DFN 272A
SPENG

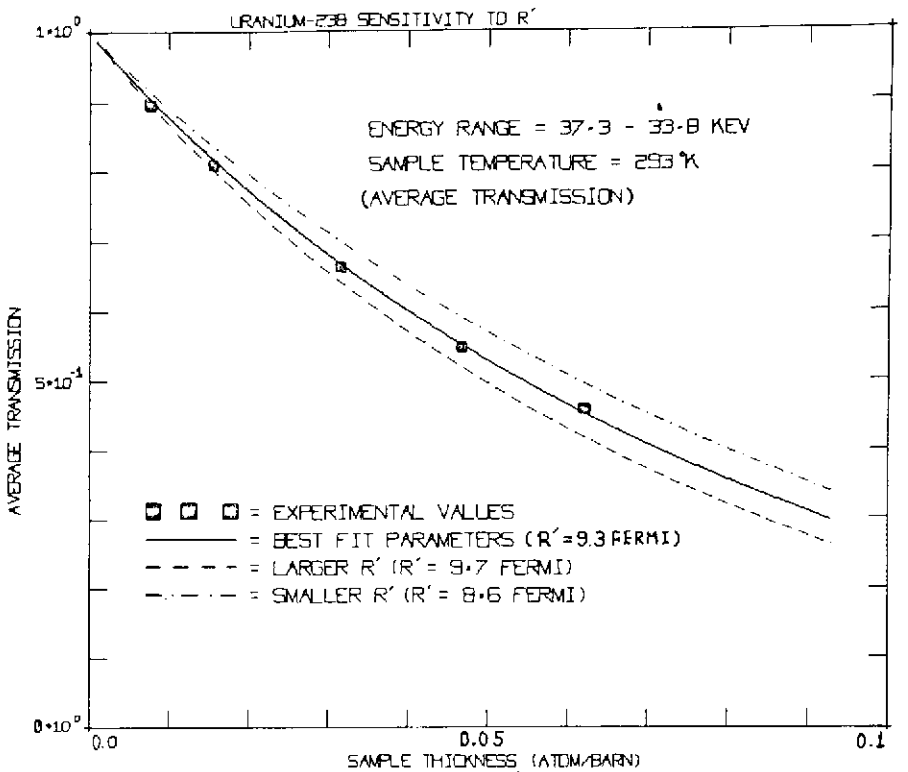
URANIUM-238 SENSITIVITY TO R'
ENERGY RANGE = 37.3 - 38.8 KEV
SAMPLE TEMPERATURE = 293°K
(AVERAGE TRANSMISSION)
= EXPERIMENTAL VALUES
= BEST FIT PARAMETERS (R'=9.3 FERMI)
= LARGER R' (R'= 9.7 FERMI)
= SMALLER R' (R'= 8.6 FERMI)
AVERAGE TRANSMISSION
1.0
5.0⁻¹
0.0
0.0
0.05
0.1
SAMPLE THICKNESS (ATOM/BARN)

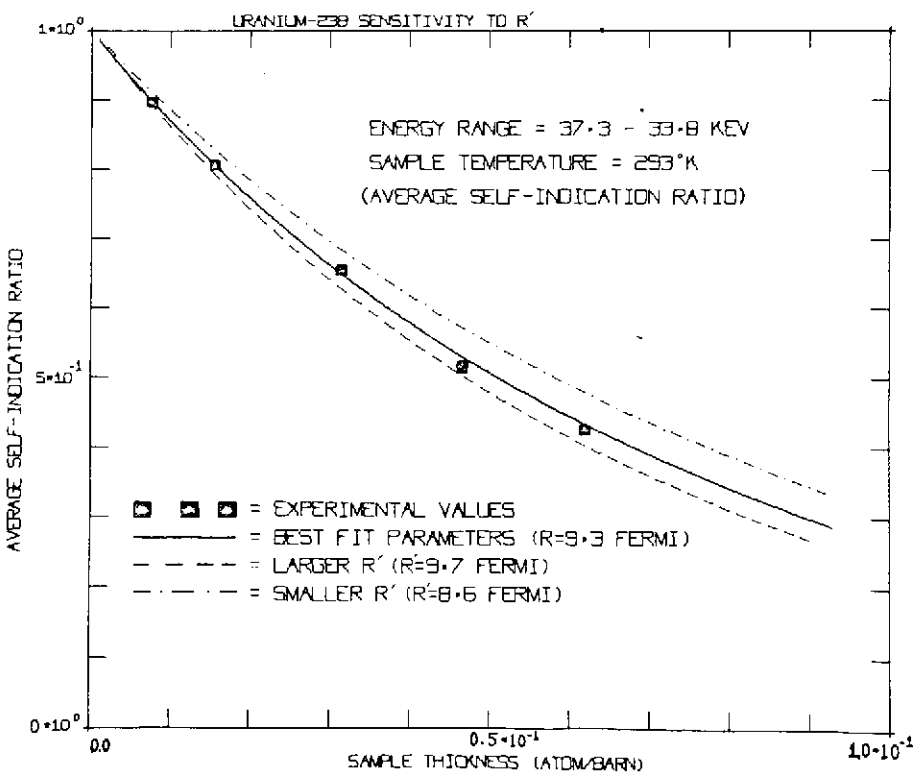
URANIUM-238 SENSITIVITY TO R'
ENERGY RANGE = 37.3 - 38.8 KEV
SAMPLE TEMPERATURE = 293°K
(AVERAGE SELF-INDICATION RATIO)
= EXPERIMENTAL VALUES
= BEST FIT PARAMETERS (R=9.3 FERMI)
= LARGER R' (R'=9.7 FERMI)
= SMALLER R' (R'=8.6 FERMI)
AVERAGE SELF-INDICATION RATIO
1.0
5.0⁻¹
0.0
0.0
0.5·10⁻¹
1.0·10⁻¹
SAMPLE THICKNESS (ATOM/BARN)

Figure 4a

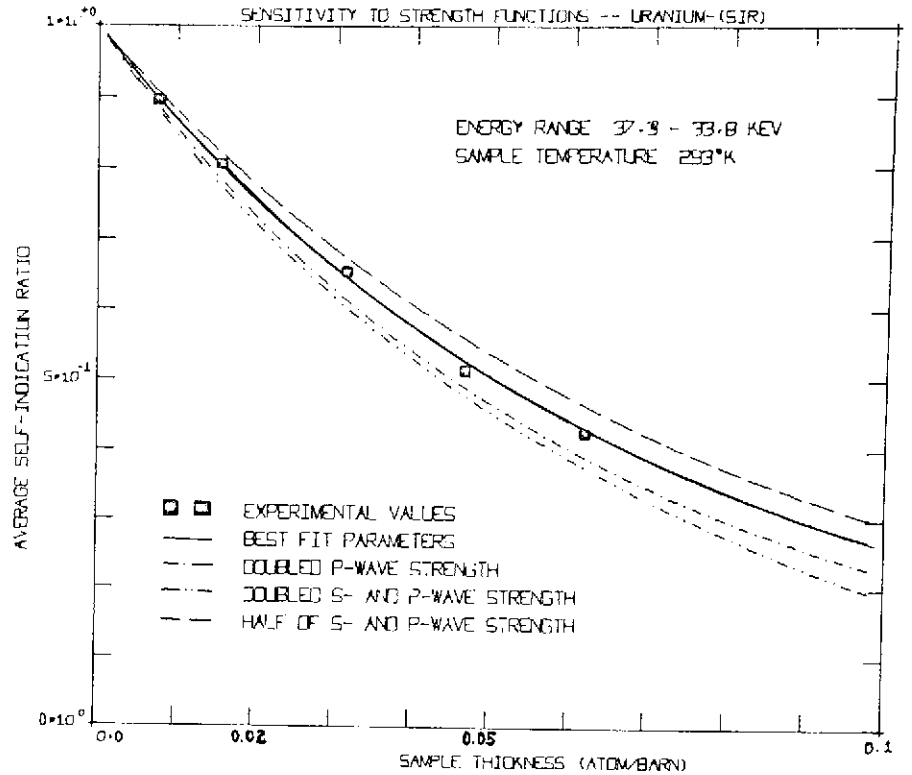
SENSITIVITY TO STRENGTH FUNCTIONS -- URANIUM-(SIR)
ENERGY RANGE 37.3 - 38.8 KEV
SAMPLE TEMPERATURE 293°K
AVERAGE SELF-INDICATION RATIO
EXPERIMENTAL VALUES
BEST FIT PARAMETERS
DOUBLED P-WAVE STRENGTH
DOUBLED S- AND P-WAVE STRENGTH
HALF OF S- AND P-WAVE STRENGTH
0.0
0.02
0.05
0.1
SAMPLE THICKNESS (ATOM/BARN)

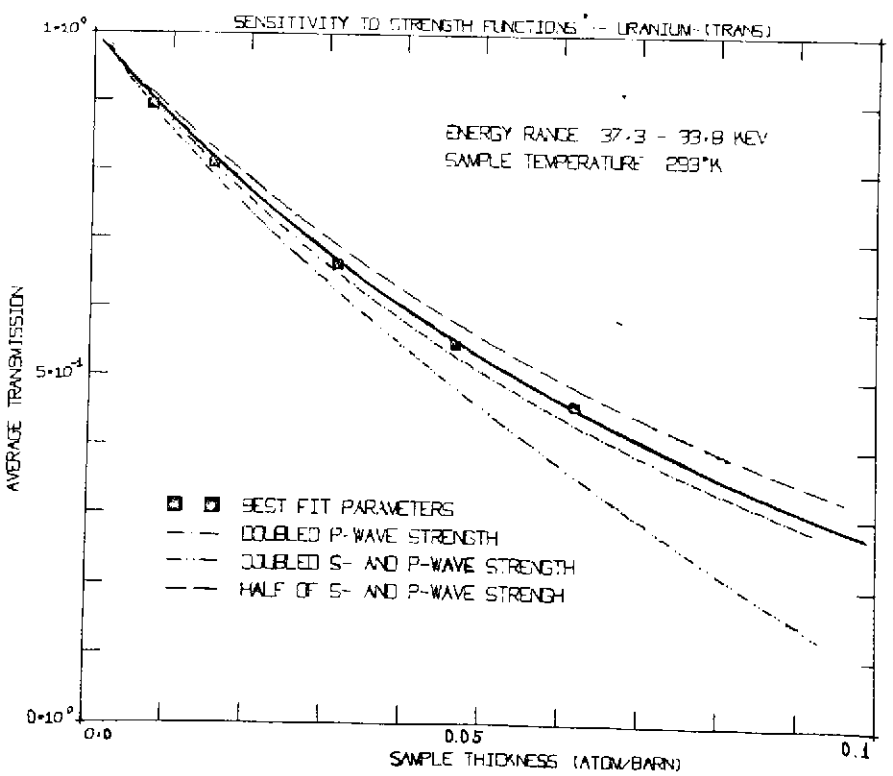
SENSITIVITY TO STRENGTH FUNCTIONS -- URANIUM-(TRANS)
ENERGY RANGE 37.3 - 38.8 KEV
SAMPLE TEMPERATURE 293°K
AVERAGE TRANSMISSION
BEST FIT PARAMETERS
DOUBLED P-WAVE STRENGTH
DOUBLED S- AND P-WAVE STRENGTH
HALF OF S- AND P-WAVE STRENGH
0.0
0.05
0.1
SAMPLE THICKNESS (ATOM/BARN)

Figure 4b

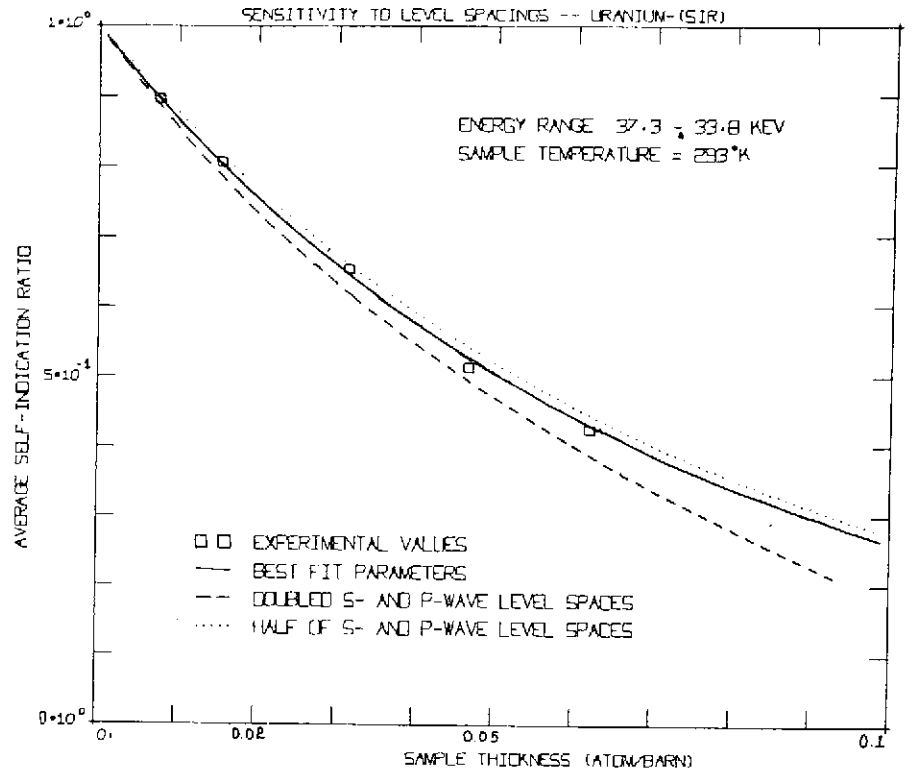
SENSITIVITY TO LEVEL SPACINGS -- URANIUM-(SIR)
ENERGY RANGE 37.3 - 38.8 KEV
SAMPLE TEMPERATURE = 293°K
AVERAGE SELF-INDICATION RATIO
EXPERIMENTAL VALUES
BEST FIT PARAMETERS
DOUBLED S- AND P-WAVE LEVEL SPACES
HALF OF S- AND P-WAVE LEVEL SPACES
SAMPLE THICKNESS (ATOM/BARN)

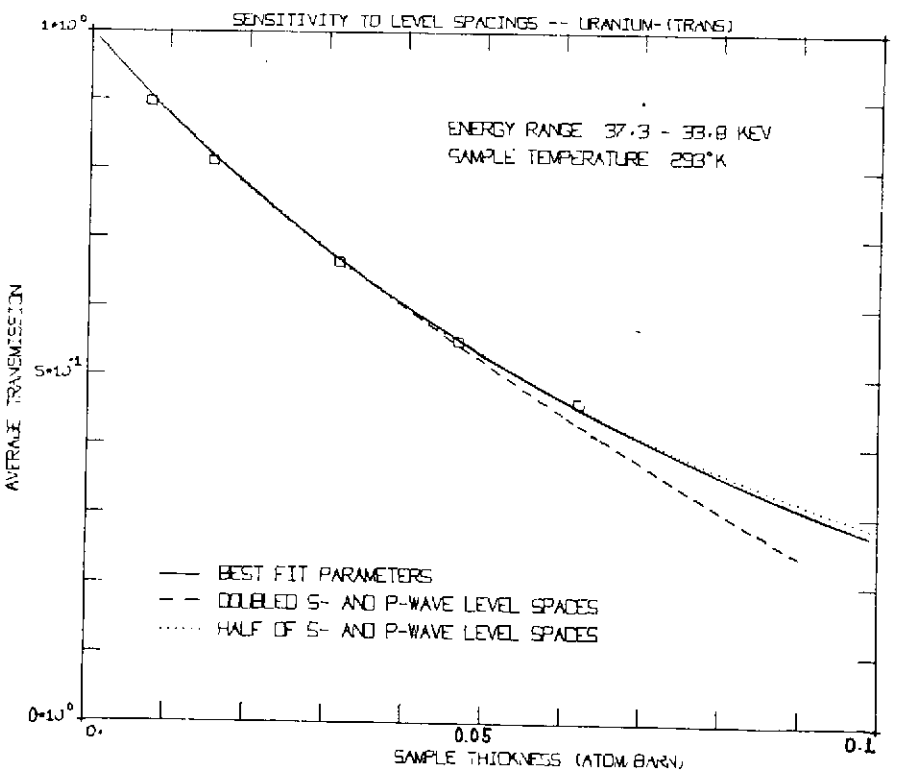
SENSITIVITY TO LEVEL SPACINGS -- URANIUM-(TRANS)
ENERGY RANGE 37.3 - 38.8 KEV
SAMPLE TEMPERATURE 293°K
AVERAGE TRANSMISSION
BEST FIT PARAMETERS
DOUBLED S- AND P-WAVE LEVEL SPACES
HALF OF S- AND P-WAVE LEVEL SPACES
SAMPLE THICKNESS (ATOM/BARN)

Figure 4c

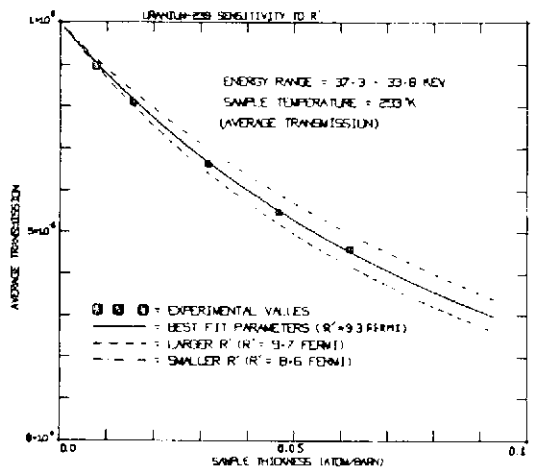

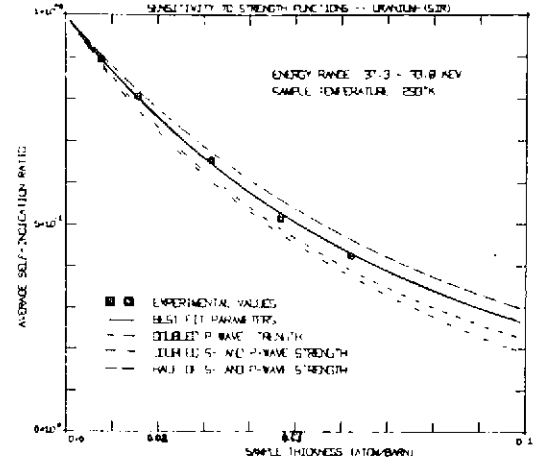

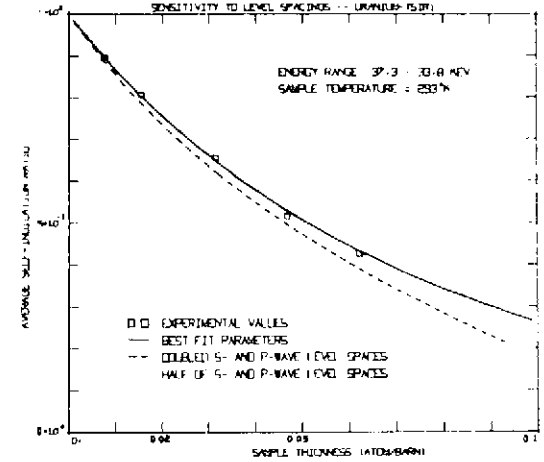

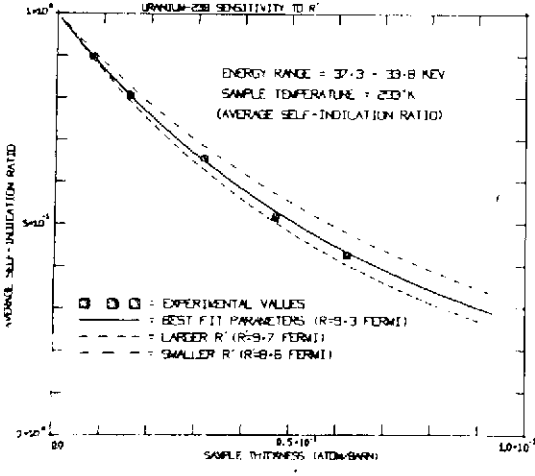

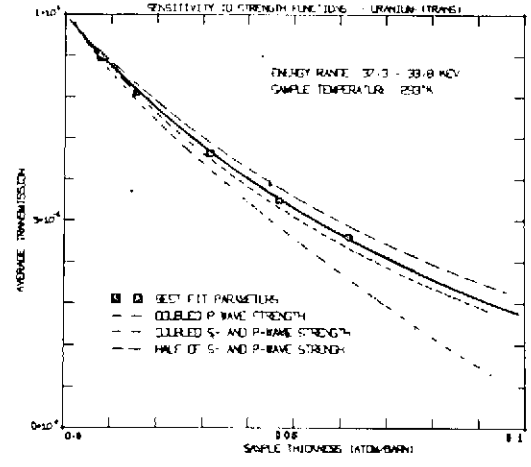

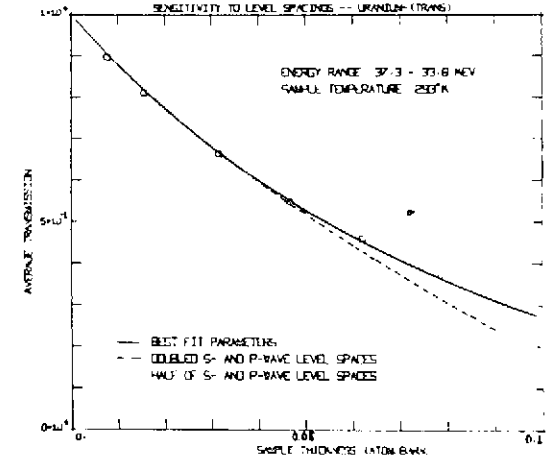

Figure 4a

Figure 4b

Figure 4c

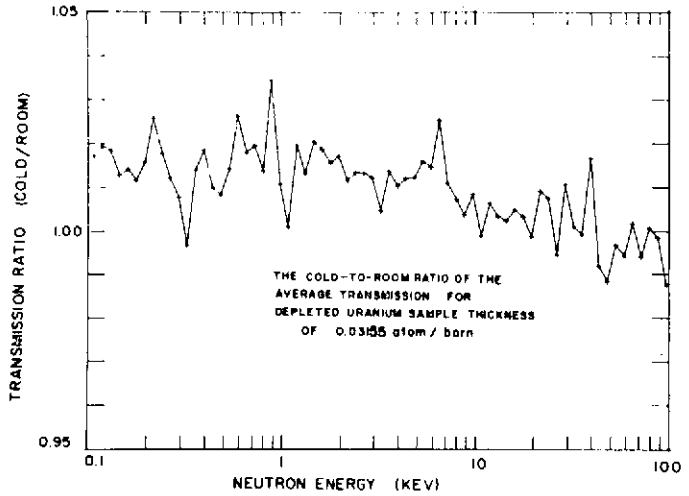

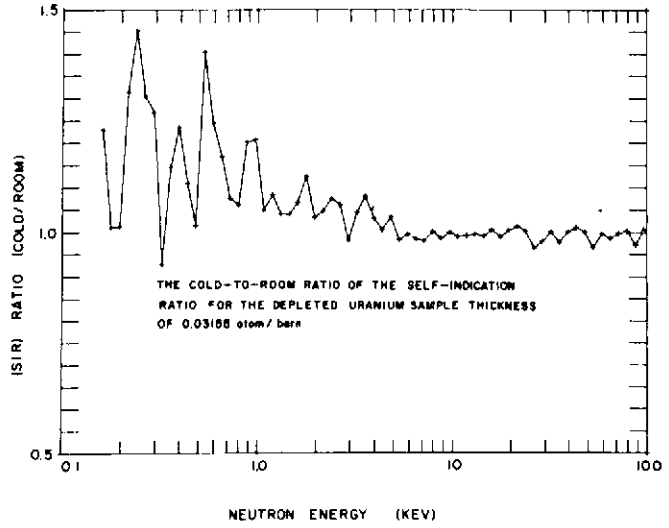

Figure 5a

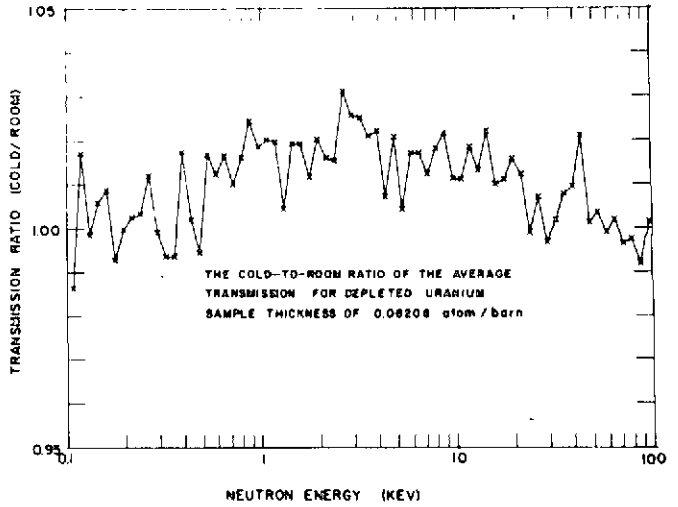

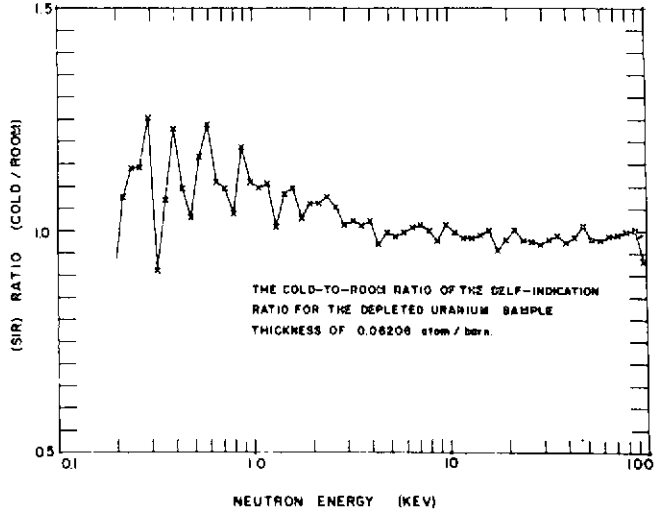

Figure 5b

Figure 9a

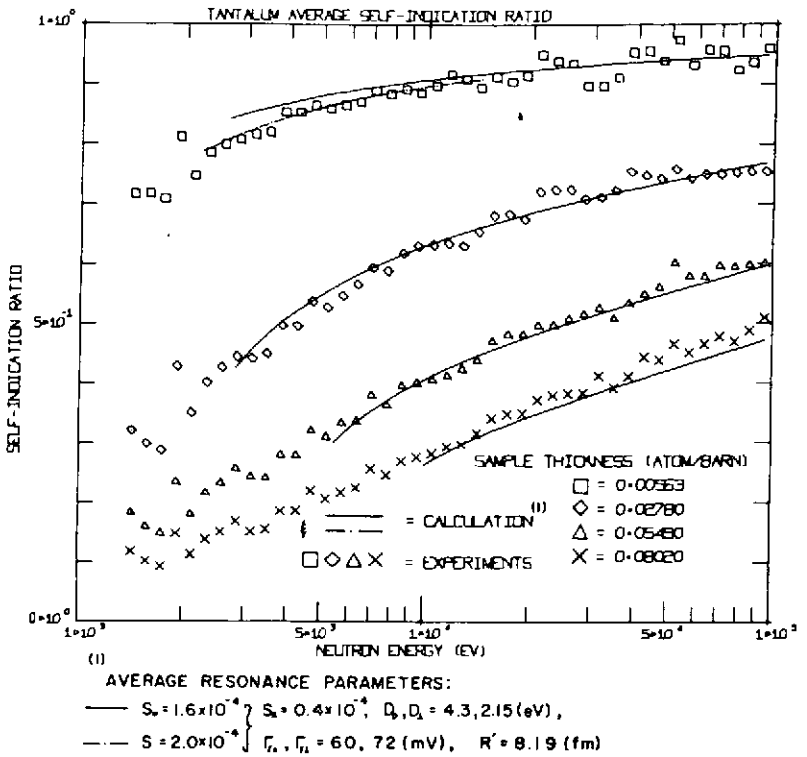

Figure 9b

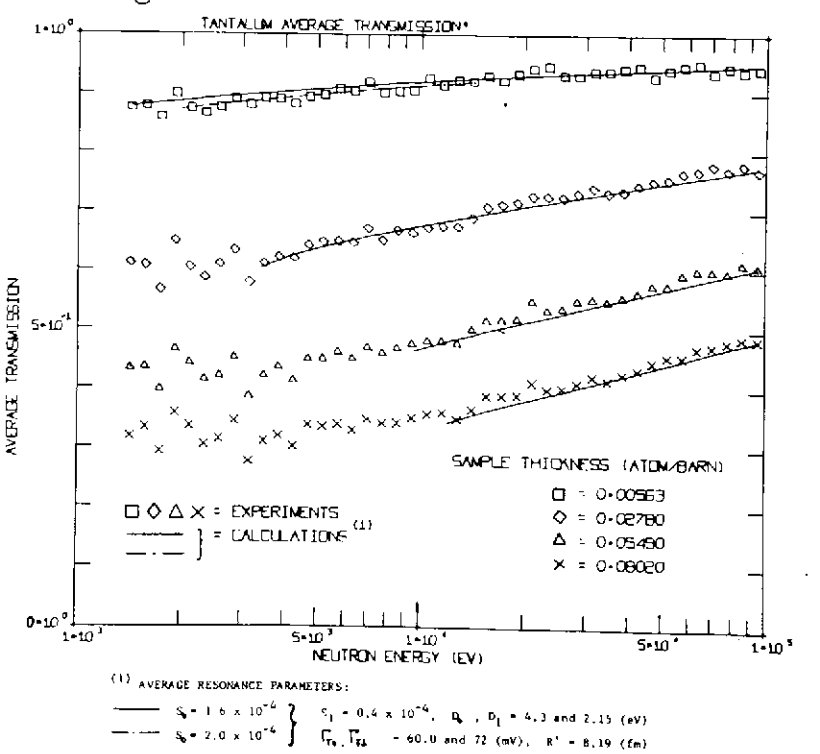

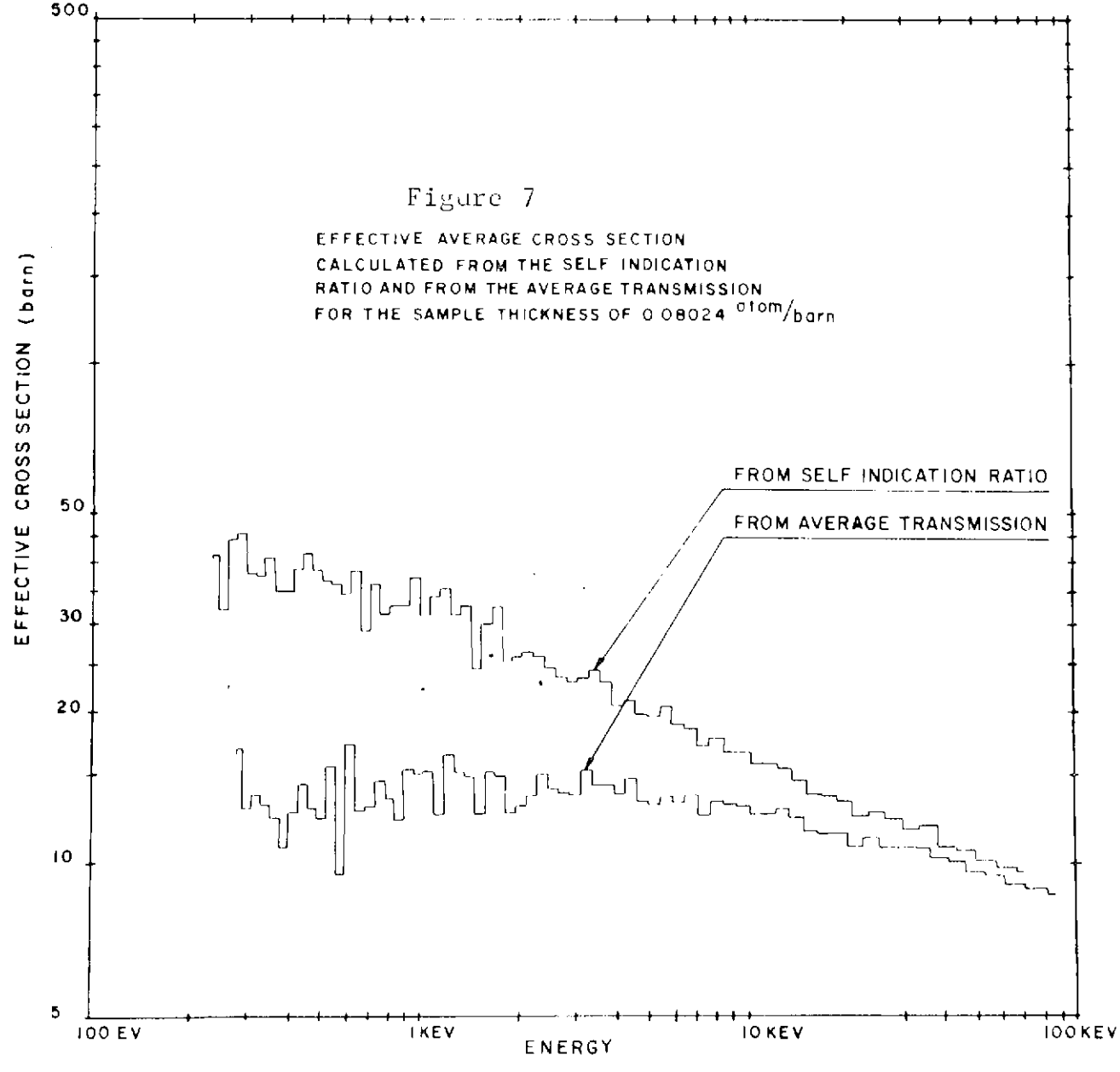

Figure 7

EFFECTIVE AVERAGE CROSS SECTION
CALCULATED FROM THE SELF INDICATION
RATIO AND FROM THE AVERAGE TRANSMISSION
FOR THE SAMPLE THICKNESS OF 0.08024 atom/barn

TABLE CAPTIONS

Table I The Best-Fit Average Resonance Parameters of ^{238}U.

Table II Comparison of the Ideal Gas Model and the Lamb Effective Temperature Model.

Table III The Cold-to-Room (and Room-to-Hot) Ratios of Depleted U <TR> and <SIR>.

Table IV The Best-Fit Average Resonance Parameters of Tantalum.

Table I. Best-Fit P-wave Strength Functions for ^{238}U for Different Scattering Lengths

	Best Fit Parameters*			ENDF/B-III	
	(A)	(B)	(C)	(D)	(E)
$S_1(10^{-4})$	$1.58^{+0.1}_{-0.1}$	$1.94^{+0.1}_{-0.2}$	$2.40^{+0.1}_{-0.2}$	1.75	1.27
$\langle D_1 \rangle$ (eV)	$11.3^{-2.0}_{+2.0}$	$11.3^{+3.5}_{+3.0}$	$11.3^{-2.0}_{+3.0}$	6.67	6.90
$\overline{\Gamma}_{\gamma 1}$(meV)	$47.5^{-8.4}_{+8.4}$	$43.8^{-13.6}_{+11.6}$	$37.0^{-6.6}_{+9.8}$	23.5	28.0
R′ (fm)	9.30	9.20	9.0	9.20	9.60
R (fm)	8.74	8.74	8.4	8.4	8.74
R^{∞}	-0.065	-0.053	-0.071	-0.095	-0.098
$S_0(10^{-4})$	1.0			1.05	1.0
$\langle D_0 \rangle$ (eV)	20.7			20.0	20.7
$\overline{\Gamma}_{\gamma 0}$ (meV)	23.0			23.5	23.0

*The uncertainties given for S_1, $\langle D_1 \rangle$, and $\overline{\Gamma}_{\gamma 1}$ correspond to the values which yield the average difference between the experimental values, R_i^{exp}, and theoretical values, R_i^{cal}, as follows:

$$\left| \overline{\Delta R} \right| = \left| \frac{1}{N} \sum_{i=1}^{N} (R_i^{exp} - R_i^{cal}) / \delta R_i^{exp} \right| \leq 2.0$$

where δR_i^{exp} denotes the statistical counting errors of the results.

Table II. Depleted-Uranium <TR> and <SIR> Calculated from Ideal Gas Model and from the Effective Temperature Theory

Energy Range = 30.6 - 27.7 keV
Sample Temperature = 77°K
Sample Thickness = 0.03155 at/b

	<TR>	<SIR>
Experimental Values	0.658 ±0.007	[illegible]
Effective Temp. Theory	0.659	[illegible]
Ideal Gas Model	0.661	[illegible]

Table III. Cold-to-Room (and Room-to-Hot) Ratios of Depleted-Uranium <TR> and <SIR> in Typical Energy Regions

Energy Regions (keV)	Sample Thickness (at/barn)	Cold-to-Room Ratio *		Room-to-Hot Ratio *	
		<TR>	<SIR>	<TR>	<SIR>
0.2-0.3	0.03155	1.019(4) # (1.016) +	1.215(9) (1.212)	1.026(4) (1.006)	1.293(8) (1.268)
	0.06206	1.008(3) (1.003)	1.076(5) (1.071)	1.030(4) (0.989)	1.350(12) (1.294)
1.0-2.0	0.03155	1.017(3) (1.015)	1.077(5) (1.075)	1.035(3) (1.017)	0.986(4) (0.969)
	0.06206	1.021(3) (1.017)	1.078(3) (1.073)	1.048(2) (1.014)	1.094(4) (1.055)
20.-30.	0.03155	1.005(3) (1.003)	0.995(5) (0.993)	1.007(3) (0.997)	0.977(5) (0.962)
	0.06206	0.996(6) (0.993)	0.985(4) (0.982)	1.006(3) (0.975)	0.993(6) (0.962)

* Sample temperatures are 77, 295 and 973°K.

\# The number, 1.019(4), stands for the ratio,

$$\langle TR \rangle^{cold} / \langle TR \rangle^{room} = 1.019 \pm 0.004 \text{ (statistical error only)}$$

and this value is for the ratio after the samples are corrected for thermal expansion.

\+ The values inside the parentheses are the ratios before the sample thickness corrections.

Table IV. Best-Fit Average Resonance Parameters of Tantalum in the Energy Range from 10 to 100 keV

	S-wave (ℓ=0)	P-wave (ℓ=1)
Strength Function (10^{-4})	$1.6\ ^{+0.3}_{-0.2}$ *	$0.4\ ^{-0.2}_{+0.3}$
Level Spacing (eV)	$4.3\ ^{-0.5}_{+1.5}$	$2.15\ ^{-0.25}_{+0.75}$
Radiation Width (meV)	$60.0\ ^{-5.0}_{+3.5}$	$72.0\ ^{-9.0}_{+6.0}$
Scattering Length R′ (fermi)	8.19 #	

*The error limitations given for all the parameters correspond to the values which yield the average difference between the experimental values, R_i^{exp}, and theoretical values, R_i^{cal}, as follows:

$$\left|\overline{\Delta R}\right| = \frac{1}{N}\left|\sum_{i=1}^{N} (R_i^{exp} - R_i^{cal})/\delta R_i^{exp}\right| \leq 2.5$$

where δR_i^{exp} denotes the statistical counting errors of the results.

#It is assumed that the channel radius R is the same as R′, that is, $R^{\infty} = 0.0$.